FLEXURAL BEHAVIOR OF HIGH-STRENGTH STEEL FIBER-REINFORCED CONCRETE COLUMNS AND STEEL-JACKETED COLUMNS

A.Suzuki [1], Y.Masuda[2], R.Yoshida[3], Y.Koshiro[4]

[1] *Obayashi Corporation, Technical Research Institute, Engineer, M.Eng, suzuki.ayaka@obayashi.co.jp*
[2] *Obayashi Corporation, Technical Research Institute, Senior Engineer, D.Eng, masuda.yasuhiko@obayashi.co.jp*
[3] *Obayashi Corporation, Technical Research Institute, Chief Research Engineer, M.Eng, yoshida.risa@obayashi.co.jp*
[4] *Obayashi Corporation, Technical Research Institute, Senior Engineer, D.Eng, koshiro.yasumichi@obayashi.co.jp*
...

Abstract

In the structural design of high-rise reinforced concrete buildings, high strength concrete is used in lower-story columns. Previous experimental studies have shown that high strength reinforced concrete columns experience brittle fractures and fail rapidly because of splitting and spalling of the cover concrete. To prevent this failure, steel fibers are added to column concrete or a steel jacket is wrapped around the column. To evaluate the flexural behaviors of these columns, a lateral loading test was carried out using columns with a strength of 150 MPa. The investigated parameters were: 1) volumetric ratio of steel fibers, 2) the presence of steel jacketing, 3) the shear span to effective depth ratio (a/d), and 4) axial force. Steel fibers were added to concrete in volume fractions of 0.5% or 1.0%. A specimen was wrapped at the top and bottom of the column with 3.2-mm-thick steel jackets of length equal to the column depth. The shear span-to-depth ratio (a/d) is 2 or 4. Specimens with the shear span-to-depth ratio of 4 simulated the behavior of columns at the first story of high-rise buildings. The test results showed the advantage of steel-fiber reinforced concrete column and steel jacketed columns in terms of sheer force and damage control. These columns showed a stable hysteretic behavior up to the drift angle of 0.05 rad. The elastic stiffness and the cracking moment were evaluated satisfactorily by the current design formula. The secant stiffness was calculated accurately by referring to previous research and evaluating the effect of the axial load. Considering the strain-softening of steel-fiber concrete, we evaluated the yield strength and the maximum strength by fiber modeling analysis. Furthermore, we observed a bond slip of reinforcement bars from stab concrete, which might have been caused by the increase of bond strength of steel-fiber concrete. It is important to evaluate the bond strength accurately when designing columns connected to beam-column joints in which the strength of concrete is lower than in the columns.

Keywords: reinforced concrete, column, high-strength concrete, steel fiber, steel jacketing

1. Introduction

Recently, several high-rise buildings have utilized concrete with a compressive strength exceeding 100 MPa, in the construction of columns. In Japan, strengths of up to 200 MPa have been successfully used in building construction. The increasing use of high-strength concrete column has raised concerns over the applicability of current building code requirements for the design and detailing of these columns. For concrete with a compressive strength greater than 70 MPa, previous experimental data was summarized in ACI 441-R. However, in Japan, current building code addressed the compressive strength of up to 60 MPa.

Previous experimental studies showed that high strength reinforced concrete (RC) columns experienced brittle fractures and failed rapidly following spalling of the cover concrete[1]. To prevent this failure, steel fibers are added to the column concrete or a steel jacket is wrapped around column. To evaluate the flexural behavior of these columns, a lateral loading test was carried out using columns with a strength of 150 MPa.

2. Experimental Investigation

2.1 Test specimens

The experimental study consisted of lateral loading tests on five RC columns with various parameters. Concrete with a target compressive strength f_c' of 150 MPa was used. The specifications of the columns are given in Table 1. The specimens had a cross section of 350 × 350 mm, and the length from the face of the stub to the end, or shear span, was a = 1400 mm. All specimens were designed that flexural failure precede other failures in accordance with AIJ (Architectural Institute of Japan) code. The specimen matrix included 1) the volumetric ratio of steel fibers, 2) the presence of steel jacketing, 3) the shear span to effective depth ratio (a/d), and 4) axial force. Steel fibers were added to concrete in volume fractions of 0.5% or 1.0%. A specimen was wrapped at the top and bottom of the column with 3.2-mm- thick steel jackets of a length equal to the column depth. The shear span-to-depth ratio (a/d) was 2 or 4. Specimens with the shear span-to-depth ratio of 4 simulated the behavior of columns at the first story of high-rise buildings. All specimens had twelve 19 mm longitudinal bars, and these main bars were welded to the end plates. The main reinforcing bars and ties had a specified yield strength of 490 and 685 MPa, respectively. Figure 1 shows the elevation and cross-sectional details of the columns together with the locations of the ties. To avoid bond splitting failure, the reinforcement ratio p_w ($p_w = a_w / bx$, a_w: cross-sectional area of a pair of reinforcements, x: interval between reinforcements

Table 1 – Experimental Tests

No.	F120-SF10-2c	F120-SF05-2c	F120-PL00-2c	F120-SF10-4c	F120-SF05-4c
f_c' [N/mm^2]	150				
b×D [mm]	350×350				
Shear span to effective depth ratio (a/d)	2			4	
η	0.4			0.15	
Longitudinal bar	12-D19(SD490) (p_g=2.81%)				
Reinforcement ratio	目-D10@50 (SD785) (p_w=1.63%)			目-D10@80 (SD785) (p_w=1.01%)	
Volumetric ratio of steel fibers [%] *	1.0	0.5	0.0	1.0	0.5

*fibers were compounded with the outer percentage

2

b: width of section) was set to a larger value than that of the actual ratio. The experimental matrix was the steel fiber mixing ratio, the shear span to effective depth ratio (a/d), and axial force. The test specimens consisted of five specimens, three specimens (F120-SF10-2c, F120-SF10-2cL, F120-SF10-4c) and two specimens (F120-SF05-2c, F120-SF05-4c), respectively, with the volume mixing ratios of steel fibers at 1.0% (80 kg/m^3) and 0.5% (40 kg/m^3). In addition to determining the basic flexural behavior, specimens with a/d=4 were also planned to simulate the behavior of columns at the first story of high-rise buildings, in which the inflection point of the first-story columns of a high-rise building tended to be higher than the capital. Three specimens were tested under high axial force ($\eta = 0.4$, η: axial force ratio ($= N / bDF_c$), N: axial force, b: column width, D: column width, F_c: target compressive strength) and two specimens were tested under low axial force ($\eta = 0.2$). In addition, since the beam-column joint on the basement floor (where the first-floor columns were attached) was generally lower in strength than the first-floor column concrete, the concrete strength of the stub was set to F_c 80 MPa, and the bond slip between longitudinal bars and the stub was also focused.

These specimens were subjected to a constant axial load and to a repeated lateral displacement sequence as shown in Figure 2. Actual testing started with the application of full axial load followed by the application of lateral load using the displacement history, as shown in Figure 3.
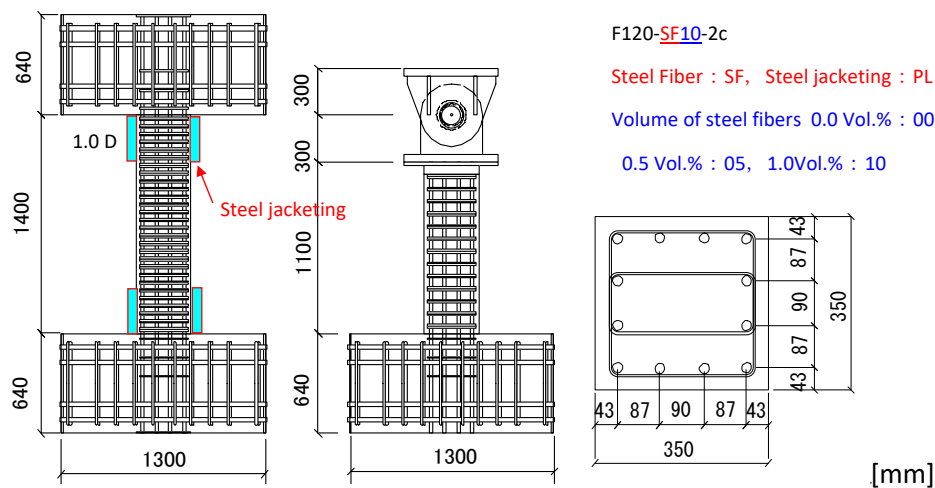

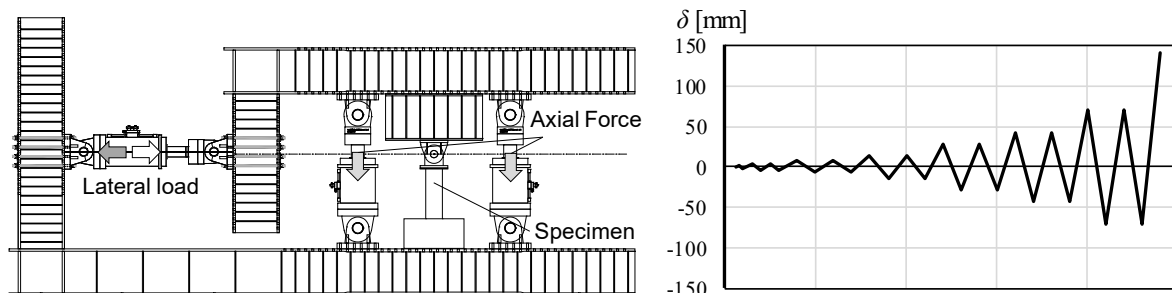Figure 1 –Elevation and cross-section of RC columns

Figure 2 – Experimental setup

Figure 3 – Displacement history

3

Table 2 – Concrete ([N/mm^2])

	Compressive Strength σ_B	Modulus of Elasticity E_c	Splitting Tensile Strength
F120-SF10-2c	158	4.96×10^4	9.80
F120-SF05-2c	163	4.50×10^4	8.56
F120-SF10-2cL	148	4.95×10^4	10.5
F120-SF10-4c	155	5.00×10^4	7.67
F120-SF05-4c	171	5.06×10^4	10.4
Stab	101	4.57×10^4	—

Table 3 – Steel ([N/mm^2])

Grade	Yield Strength σ_y	Tensile Strength σ_t	Modulus of Elasticity E_s
D19 (SD490)	524	692	1.98×10^5
D10 (SD785)	858	1056	2.15×10^5

Table 4 – Fiber ([N/mm^2])

	Form	Diameter [mm]	Length [mm]	Gravity [g/cm^3]	Yielding Strength [N/mm^2]
SF	Fuck	0.62	30	7.85	1190

SF :

2.2 Test results

Figure 4 shows the lateral load Q_c and displacement δ. Figure 5 shows the comparison of the Q_c -δ curve by the steel fiber mixing ratio for each a/d, and Table 5 lists the experimental results. Here, the lateral load Q_c is a value obtained by correcting the lateral force due to the inclination of the vertical actuator.

(1) Steel Fiber Specimens

In the cycle of R = 2.5 × 10^{-3} rad, flexural cracks occurred at the top and bottom of the column (hinge zone). In the cycle of R = 5.0 × 10^{-3} rad, vertical cracks due to crushing occurred in the compression side. The longitudinal bar yielded compressively in the cycle of R = 10 × 10^{-3} rad, and reached the maximum lateral load in the cycle of R = 20 × 10^{-3} rad. In this cycle, cracks were continuously generated along the intermediate longitudinal bar over the entire section. From R = 50 to 100 × 10^{-3} rad, spalling of cover concrete progressed in the range of D / 2 from the end of the member.

The deformation properties of F120-SF10-2c and F120-SF05-2c did not widely differ up to R = 33 × 10^{-3} rad, and the maximum load was almost the same. After the point, the strength of F120-SF05-2c decreased more abruptly than that of F120-SF10-2c. This occurred because the difference in the volume mixing ratio of the steel fibers slightly affected the progress of spalling of the cover concrete. In all the test specimens, no severe spalling or an abrupt decrease in strength was observed in columns without steel fibers.

(2) Steel Jacketing Specimens

In R = 2.5 × 10^{-3} rad, flexural cracking at the top and bottoms was observed. Cracks occurred at the end of the steel plate on the compression side. The longitudinal bar was compressively yielded in the cycle of R = 1/100. The maximum strength was reached in the cycle of R = 1/50, and the longitudinal bar yielded in tension. In this cycle, small diagonal cracks were generated at the corners on the compression side. In the part without steel plate reinforcement, continuous fine diagonal cracks occurred in the cycle of R = 33 × 10^{-3} rad. In the cycle of R = 50 × 10^{-3} rad, vertical cracks occurred, and the tensile steel plate yielded and collapsed with a loud noise. As a result, the swelling at the corners greatly expanded and the maximum strength suddenly decreased. As shown in Figure 4, in the cycle of R = 20 × 10^{-3} $\sim$30 × 10^{-3} rad, the load decreased in a more
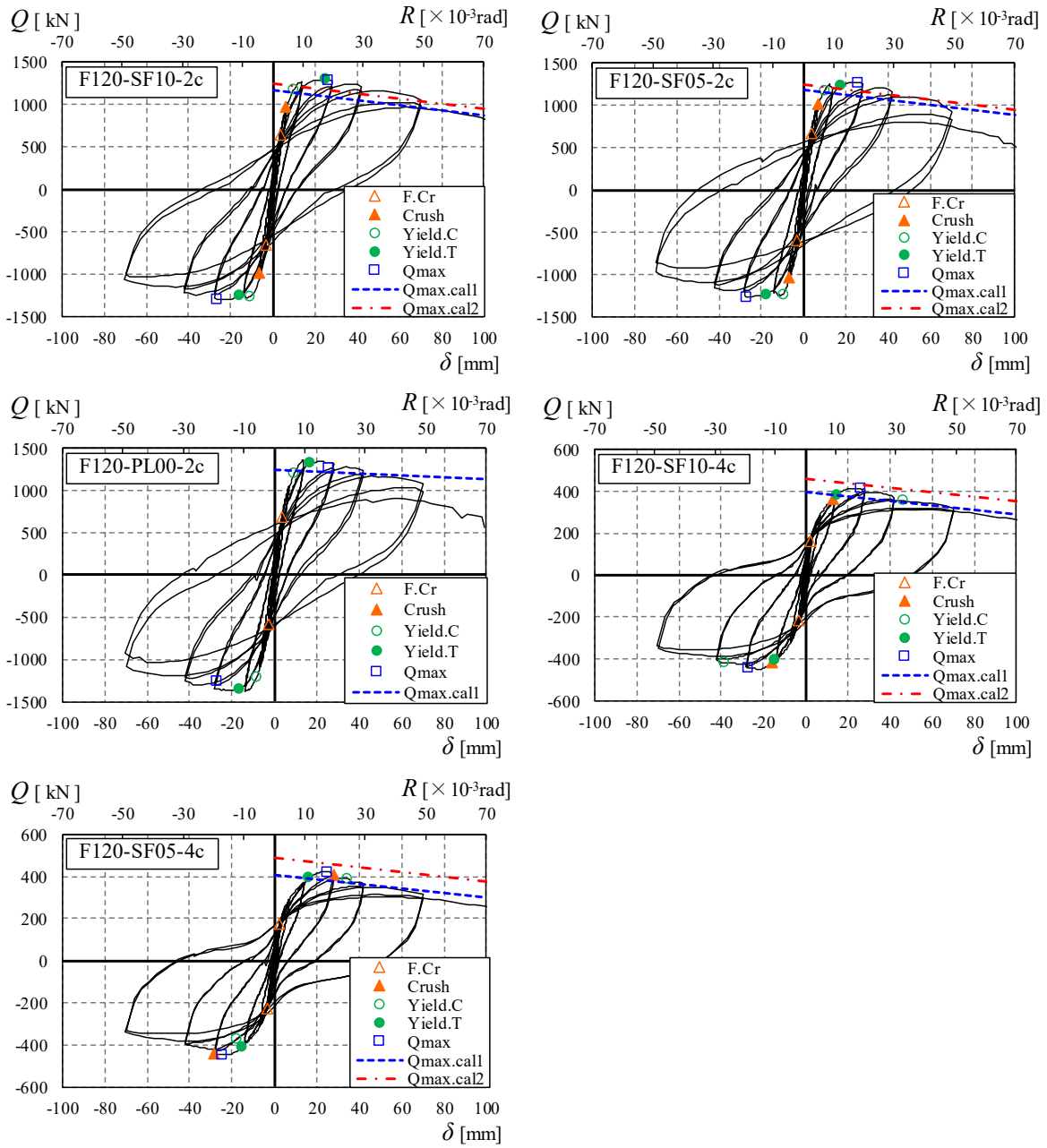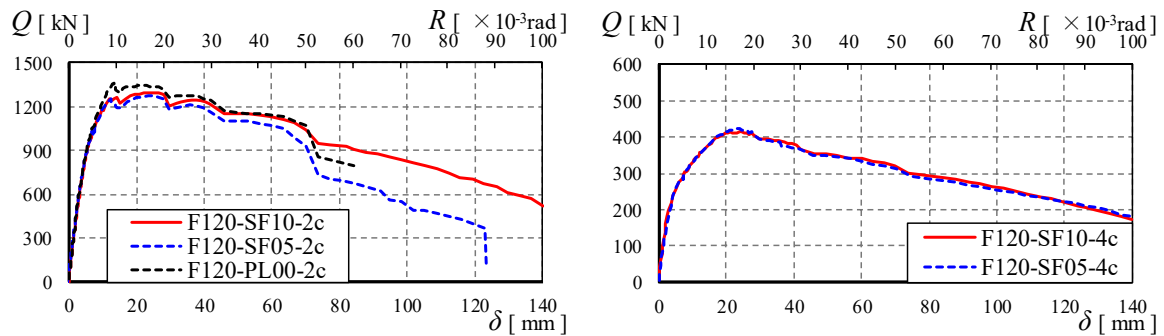
4

Figure 4 – Behavior of Specimens

Figure 5 – Effect of Steel Fibers

5

ductular fashion from the maximum strength than that of F120-SF10-2c. However, after R = 5%, although the strength was maintained, the damage due to spalling was more severe than that of the fiber specimen, and the load could not be supported after R = 7%.

(3) Specimens with the shear span-to-depth ratio (a/d) of 4

In the cycle of R = 10×10^{-3} rad, the longitudinal bar yielded tensely. The maximum load was reached in the cycle of R = 20×10^{-3} rad. The deformation properties of F120-SF10-4c and F120-SF05-4c did not widely differ until the final displacement. This is because under the conditions of the shear span ratio and the axial force ratio, the progress of the cover concrete spalling was small and the difference in the reinforcing effect by the steel fibers was not apparent. In addition, as shown in F120-SF10-2cL, after R = 33×10^{-3} rad, floating was observed on the stub concrete surface, and the hysteresis curve showed a slight slip property as compared to the specimen with a/d = 2.

2.3 Test Observations

Figure 6 shows the damage of each specimen at R = 10×10^{-3} rad and R = 50×10^{-3} rad.

(1) Steel Fiber Specimens

No significant difference was observed between the two specimens up to R = 10×10^{-3} rad. When the steel fibers' contamination ratio was high, the area of the exfoliated concrete cover caused by crushing tended to be slightly smaller.

(2) Steel Jacketing Specimens

There was no significant difference in the strength and deformation properties of the steel fiber specimens However, a different failure process was observed. At R = 20×10^{-3} rad, steel fiber specimens demonstrated peeling due to spalling of the cover concrete and diagonal cracks along the middle longitudinal bar. On the other hand, in F120-PL00-2c, bending cracks at the edge of the steel and small diagonal cracks at the corners were observed. After R = 50×10^{-3} rad, swelling in the corner with spalling of the cover concrete was greatly expanded. When the steel jacketing was removed after the fracture, there were many cracks due to compression, but a slight crushing of the cover was observed. The crushing was suppressed and restrained by the steel plate. At R = 10×10^{-3} rad, diagonal cracks occurred due to the column longitudinal bars coming out, and at R = 3.3%, the stub surface came off.

(4) Specimens with the shear span-to-depth ratio (a/d) of 4

No significant difference was observed between the two specimens up to R = 100×10^{-3} rad. In all the specimens, many bending-shear cracks were observed, and the cover concrete peeled off due to crushing in the area of the column base D / 2.

3. Discussion of Results

Table 5 shows test data and the calculated values.

3.1 Stiffness

The elastic stiffness and the secant stiffness were calculated by the AIJ design formula. The elastic stiffness was evaluated satisfactorily by not considering the effect of the steel fibers. The secant stiffness was calculated more accurately by referring to previous research and evaluating the effect of the axial load. References 2) and 3) showed that the stiffness reduction at yielding α_y is affected more by the axial force ratio in ultra-high strength concrete than in normal strength concrete.

6

Here, for the concrete compressive strength $\sigma_B = 55$ to 168 MPa when the shear span ratio was less than 2, equation (1) showed that when the coefficient of the axial force ratio η term in the previous equation[4] was increased from 0.169 to 1.97, it matched well with the experimental values. Therefore, the same equation was used for evaluation in this experiment. When the shear span ratio was 2 or more, it was assumed that the stiffness reduction at yielding α_y was also affected by the axial force ratio, and the coefficient of the axial force ratio η term was set to the value that was equal to the value determined by equation (1) at a/d = 2. Thus, the coefficient of the term of the axial force ratio η in the previous equation[4] was increased from 0.33 to 2.32, and equation (2) was derived.

・a/d $\leqq$ 2

$$\alpha_y = \left(-0.0836 + 0.159 \cdot (M/QD) + 1.97 \cdot \eta_o\right) \cdot (d/D)^2 \tag{1}$$

・a/d $>$ 2

$$\alpha_y = \left(0.043 + 1.64 np_t + 0.043 \cdot (M/QD) + 2.32 \cdot \eta_o\right) \cdot (d/D)^2 \tag{2}$$

Table 5 – Test Results

Specimen		F120-SF10-2c		F120-SF05-2c		F120-PL00-2c		F120-SF10-4c		F120-SF05-4c	
Elastic stiffness [kN/mm]	Exp	189		181		202		71.1		67.6	
	Cal	184		185		184		73.4		74.2	
	Exp/Cal	1.03		0.98		1.1		0.97		0.91	
Flexural Crack Moment [kN・m]	Exp	466		485		498		114		128	
	Cal	438		438		438		97		99	
	Exp/Cal	1.07		1.04		1.13		1.39		1.47	
Maximum Moment [kN・m]	Exp	985	-988	968	-965	1015	-1030	316	-340	323	-340
	Cal1.ε_{cu}	823 (1.19)		827 (1.17)		873 (1.17)		278 (1.18)		285 (1.16)	
	Cal2.ε_{cu}	878 (1.12)		874 (1.10)		—		323 (0.98)		340 (0.94)	
Yield Moment [kN・m]	Exp	850	-915	853	-888	874	-869	299	-298	309	-279
	Cal1.ε_{cu}	1092 (1.15)		1121 (1.11)		1210 (1.16)		337 (1.23)		1171 (1.06)	
	Cal2.ε_{cu}	1181 (1.05)		1176 (1.03)		—		404 (1.05)		428 (1.03)	

R=1.0%	R=5.0%	R=1.0%	R=5.0%	R=1.0%	R=5.0%	R=1.0%	R=5.0%	R=1.0%	R=5.0%
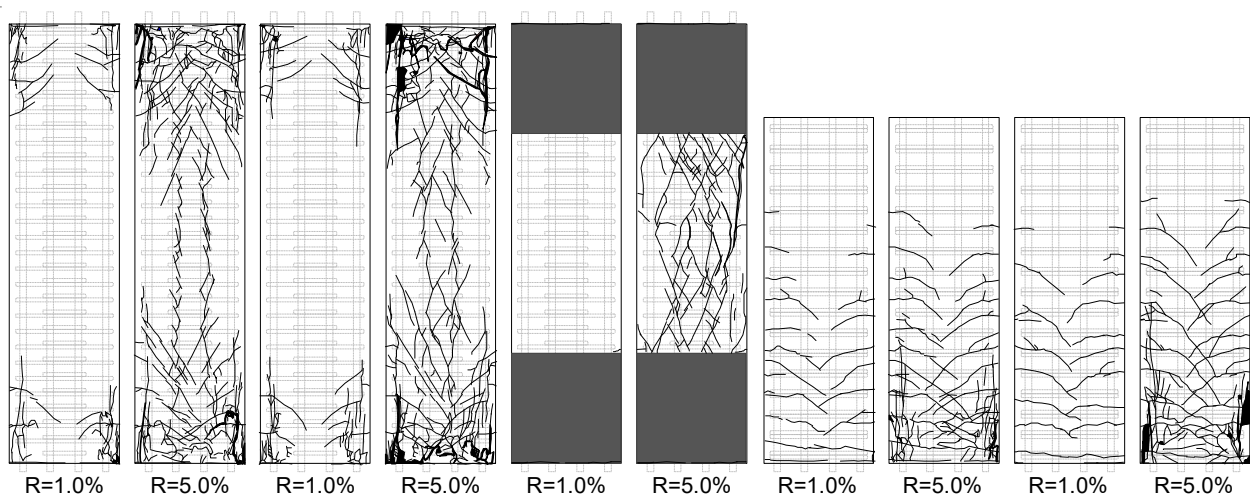
F120-SF10-2c   F120-SF05-2c   F120-PL00-2c   F120-SF10-4c   F120-SF05-4c

Figure 6 –Damage of Specimens at 10×10^{-3} rad and 50×10^{-3} rad

a/d : shear span-to-depth ratio η_o : axial force ratio $(= N/bDF_c)$

N : axial force n : modular ratio p_t : ratio of yield strength

Figure 7 shows a comparison between the experimental value and the calculated value of the stiffness reduction at yielding α_y. The experimental and calculated values were almost the same regardless of the shear-span ratio, and the proposed formula was satisfactory in its evaluation. However, α_y was over 1.0 when the axial force was large. The use of a longitudinal bar of high strength yield was also considered for evaluating α_y.

3.2 Effect of volumetric ratio of steel fibers on flexural strength

The flexural cracking strength Q_c is given by equation (3)[2]. For steel fiber specimens, the experimental and calculated values were nearly identical, and for steel rolled specimens, the experimental values were slightly higher than the calculated values.

$$Q_c = 2 \cdot (0.56\sqrt{\sigma_B} + \sigma_0) \cdot Z_e/L_0 \quad (3)$$

σ_B : Compressive strength [N/mm^2] σ_o : Axial stress [N/mm^2] N : axial force [N]

B : width [mm] D : depth [mm] Z_e : modulus of equivalent section [mm^3] L_o : clear span [mm]
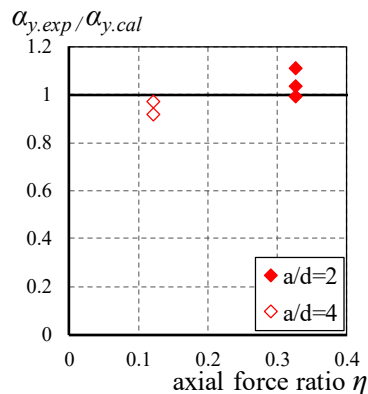

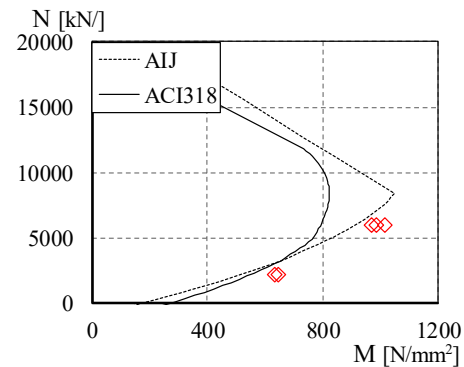Figure 7 – Relationship between α_y and η

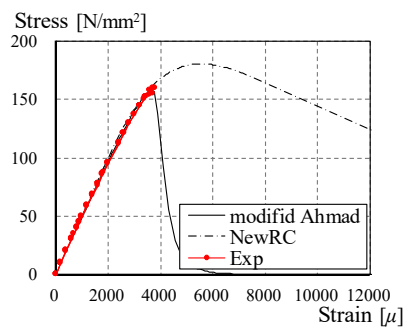Figure 8 – Relationship between M and N

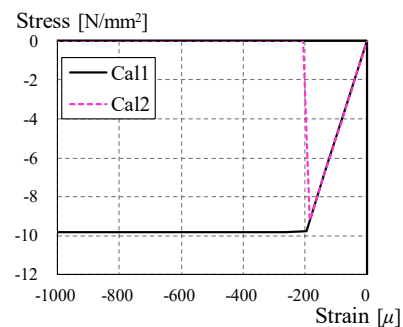Figure 9 – Stress-Strain Curve (Compression)

Figure 10 – Stress-Strain Curve (Tension)

Figure 8 shows the M-N interaction curve of the column specimens and the value calculated by the ACI code given by equation (4). Previous studies indicate that the maximum strength of high-strength concrete can be thoroughly evaluated by AIJ under high axial forces, and the values from ACI318 were approximately equal to the experimental results. In this study, the experimental value was larger than calculated value by an ACI as large as 1.2.

$$ M_u = \sum A_{st} \cdot \sigma_{st} \cdot d - \sum A_{sc} \cdot \sigma_{sc} \cdot d_c - \sigma_{av} \cdot b \cdot (\beta_1 \cdot x_n)^2 / 2 + N \cdot g \qquad (4) $$

β_1 : 0.85 ΣA_{st} : area of longitudinal tensile bar ΣA_{sc} : area of longitudinal compressive bar

σ_{st} : Tensile srength of longitudinal bar σ_{sc} : Compressive srength of longitudinal bar

d : distance from extreme compression fiber to centroid of longitudinal tension reinforcement

d_c : distance from extreme compression fiber to centroid of longitudinal compression reinforcement

σ_{av} : the intensity of stress in the stress block x_n : the depth of the stress block to the depth of the neutral

axis g : the depth of the stress block to the depth of the compressive axis

The stress drop gradient after compression and the tensile strength of the steel fiber reinforced concrete became gentle, although it was difficult to confirm these results via the material test using a test piece. Using this consideration as a variable, Cal1 and Cal2 were calculated by cross-sectional analysis using a fiber model. In Cal1, the modified Ahmad model[5] was used for the elements outside the stirrups, and the New RC model[6], which considered the constraining effect, was used for the core concrete (the element inside the steel plate in the rolled specimen). In Cal2, in consideration of the reinforcing effect of steel fiber, and in addition to the model used in Cal1, we assumed that the stress was maintained from tensile strength to ultimate strain ε_u (= 0.01). The maximum strength was the value when the strain of the extreme compression fiber was the strain at the compressive strength. Cal2 was greater than Cal1 in both the yield strength and the maximum strength. A more accurate evaluation of the stress gradient following the compressive / tensile strength is a topic for future studies.

3.3 Bond slip

When there was a difference in the concrete compressive strength between columns and stubs, the phenomenon where the main bar of the column comes out of the stub should be confirmed. The stub lifting displacement δ_s and column base opening displacement δ_c were observed. Figure 11 shows the definitions of δ_s and δ_c. The column base opening displacement δ_c was the sum of the stub lifting displacement δ_s and the column base crack width. Figure 12 shows the relationship between stub lifting displacement δ_s and horizontal displacement
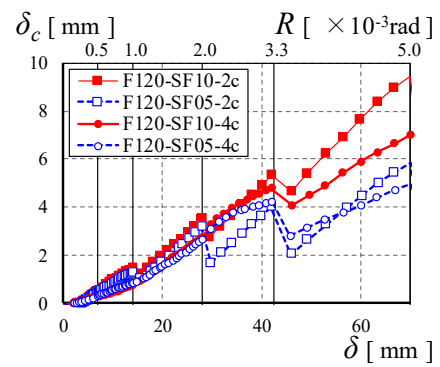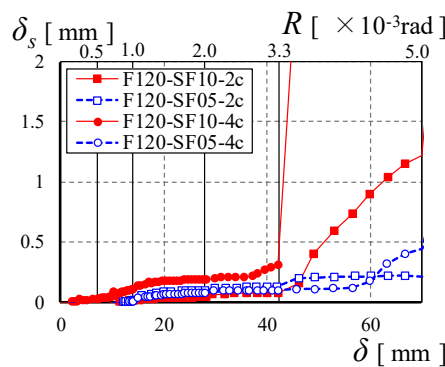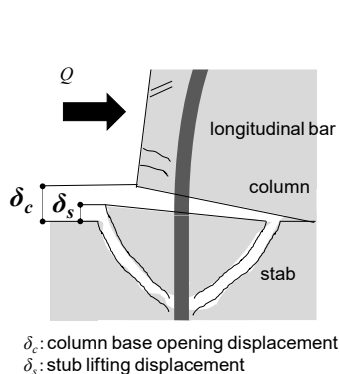

δ_c: column base opening displacement
δ_s: stub lifting displacement

Figure 11 – definition of displacement   Figure 12 – behavior of δ_s Figure 13 – behavior of δ_c

9

δ, and Figure 13 shows the relationship between column base opening displacement δ_c and horizontal displacement δ.

From Figures. 12 and 13, from $\delta = 40$ mm onwards, the higher the fiber mixing ratio, the larger the stub lifting displacement and column base opening displacement. Reference [7] reports that steel fibers improve the bond strength. Specifically, the bond performance of the longitudinal bar in the column is improved in accordance with the amount of steel fibers, and there is a possibility that the slipping of longitudinal bar of the column from the stub may come out prominently. There is a concern that this phenomenon may affect the hysteresis of the frame and damage to the beam-column joints, but further investigation is needed to quantitatively determine the amount of displacement.

4. Conclusions

Cyclic loading tests of RC columns using ultra-high strength concrete with steel fibers or steel jacketing were conducted to evaluate the flexural behavior of these columns, and the following findings were obtained.

1) The specimen with 1.0% mixed steel fibers more thoroughly suppressed spalling of the cover concrete and tended to improve the toughness compared to the specimen with 0.5%. However, in the case of a/d = 4, there was no effect on the toughness due to the difference in steel fiber content.

2) The stiffness reduction at yielding α_y of the column in this experiment was evaluated successfully by increasing the coefficient of the axial force ratio term in the existing formula.

3) Considering the strain-softening of steel-fiber concrete, we evaluated the yield strength and the maximum strength by fiber modeling analysis. A more accurate evaluation of the stress gradient following the compressive / tensile strength is a topic for future studies.

4) The concrete on the stub lifted and the main bars of the column came out of the stub. The higher the steel fiber content, the greater the displacement of the column base opening when a difference in strength was provided between the columns and stubs.

5. References

[1] Sugimoto, K., Masuda, Y., Tsuda, K., Naganuma, K., (2007): Bending shear test on RC columns using ultra high strength concrete. *The JCI annual convention*, 29 (3), 541-546.

[2] Kumazawa, Y., Maeda, H., Matsumoto, I., Sugiyama, T., Nakano, K., Matsuzaki, Y., (2001): Study on Structural Performance of Reinforced Concrete Column using High Strength Concrete and High Strength Shear Reinforcement. Annual Meeting Architectural Institute of Japan. C-2, Structures IV,433-434

[3] Okuda, M., Shikano, H., Nakano, K., Matsuzaki, Y., (2004): Experimental Study on RC Columns using 150MPa, Japan Concrete Institute 26(2), 283-288

[4] *1997/07*, Design Guidelines for Earthquake Resistant reinforced Concrete Buildings Based on Inelastic Displacement Concept, Architectural Institute of Japan

[5] Naganuma, K., (1995): Stress-Strain Relationship for Concrete Under Triaxial Compression, Journal of Structural and Construction Engineering (Transactions of AIJ) 60(474), 163-170

[6] Sakino, K., Sun, Y., (1994): Stress-Strain Curve of Concrete Confined by Rectilinear Hoop, Journal of Structural and Construction Engineering (Transactions of AIJ) 59(461), 95-104

[7] Bilal S. Hamad, Mohamad H. Harajli, and Ghaida' Jumaa, (2001): Effect of Fiber Reinforcement on Bond Strength of Tension Lap Splices in High-Strength Concrete, ACI Structural Journal, 98(5), 638-947